Journal of Applied Sciences and Nanotechnology, Vol. 2, No. 2 (2022)

Journal of Applied Sciences and Nanotechnology

Journal homepage: https://jasn.uotechnology.edu.iq/

Improvement of Substrates Properties by Incorporating Titanium Nanoparticles Deposited by DC Diode Sputtering Approach

Iman H. Hadi*, Muslim F. Jawad, Khaleel I. Hassoon

Laser Science and Technology Branch, Department of Applied Sciences, University of Technology – Iraq

Article information

Article history:
Received: August, 15, 2021
Accepted: March, 04, 2022
Available online: June, 10, 2022

Keywords:
Titanium nanoparticles,
DC diode sputtering approach,
X-ray diffraction,
FESEM

Corresponding Author:
Iman H. Hadi
iman.h.hadi@uotechnology.edu.iq

Abstract

In this work, the synthesis of titanium thin films on two different substrates (glass and n-type Si), with thicknesses of 90 and 145 nm at two different times (5 and 10 min) respectively, have been obtained. The thin films have been successfully deposited on glass and silicon substrates using DC diode sputtering technique. The optical properties of the prepared thin films have been checked out using the optical reflectance spectrum. A significant reduction in surface reflectivity was observed at (10 min) sputtering time. The structural properties of the prepared thin films were studied using X-ray diffraction (XRD) and field-emission scanning electron microscopy (FE-SEM). XRD results confirmed that titanium thin films had a hexagonal structure with preferred orientation on (002). The images of FESEM showed that all the samples had a uniform distribution of granular surface morphology. The grain sizes of the Ti nanostructure were estimated using Scherrers' analysis. The thickness of Ti thin film increased as the sputtering time increased for both glass and Si n-type substrates. The repeated experiments revealed that the most uniform Ti thin film is on Si substrate (n-type) with particle size 10 nm at deposition time 5 min.

DOI: 10.53293/jasn.2021.4069.1075, Department of Applied Sciences, University of Technology

1. Introduction

Titanium nanoparticles have gotten great attention due to their attractive characteristics. Thus, control of the structure formation during film fabrication appears to be of great importance for a particular application. Titanium has been utilized in the micro-electro-mechanical system, optoelectronic devices, bio-applications, and mechanical equipment [1–9]. Many efforts have been made to obtain (002) orientation. Among various Ti orientations, the (002) oriented Ti film was optimum for the (002) growth on Si wafers [10]. Therefore, the growth of highly (002) oriented Ti films has been an important issue in sputtering. Ti thin films have been utilized in many applications such as biomedical applications, and micro-electro-mechanical system equipment technology due to their specific characterizations like excellent biocompatibility, and good thermal and chemical stabilization [11]. Titanium thin films can be largely obtained utilizing diverse sputtering like direct current (DC) sputtering [12], radio frequency (RF) sputtering process [13], high power impulse magnetron sputtering [14], which is a familiar process in the industry to achieve thin-films with high reproducing and growth rate. DC sputtering deposition of titanium metal film in argon ambient ensures a high deposition rate. The effect of the deposition parameters like sputtering power and the separation between the cathode and the anode on the characterization and structure of titanium thin films by the DC sputtering technique has been studied by many researchers [15-20]. While few researchers have studied the deposition of titanium thin films by the RF sputtering process, RF sputtering can get a feature of a high ionization degree according to the vibrations of the electrons in the plasma [21]. Meantime, there are other

techniques like bias sputtering [22], and ion beam assisted deposition [23] to set ions energy in the plasma since the substrate influences the deposition properties of thin films. However, an electric bias in these techniques would be used toward the anode, which can overlap within the plasma or require complicated and costly requirements. So the DC sputtering technique can be considered a simple and low cost to obtain metal's and alloy's thin films [24]. In the physical vapor deposition (DC sputtering process), an electron is accelerated from the cathode toward the argon atom and collide with it to produce the argon ion, this ion has a positive charge, so it will attract toward the cathode to eject an atom from the target toward the substrate. This process will be repeated many times until the thin film is formed [25]. Plasmonics includes the sciences and applications of noble metal structures that lead and influence visible light at nanoscale lengths—much smaller structures than the light wavelength [26]. Plasmonics is predicted to be the key nanotechnology to merge electronic and photonic elements on the same chip [27]. The plasmonic characteristics are responsive to change in the local insulation environment, that is at present associated with the size, shape, and spacing of the utilized metal nanostructures [28]. Establishing metal nanostructures for optoelectronic devices can be the most hopeful way to improve the device's performance while keeping the same size [29, 30]. Till now, very large advances have been made towards plasmonic improved optoelectronic devices, for example, in solar cells [31], photodetectors [32], and LED'S [33]. In the current work, titanium nanoparticles have been deposited on glass and n-type silicon substrates via DC sputtering technique then investigated the sputtering time effect on the particle formation.

2. Experimental Work

A schematic diagram of the DC sputtering system is shown in Figure 1. Titanium disc of 4.7 cm diameter and 5mm thickness with 99.9% purity supported from SIGMA-ALDRICH has been located on the cathode in the sputtering chamber. Glass and n-type Si (111) with 5–40 Ω cm resistivity and 0.45 mm thickness have been used as substrates for the deposition, these substrates with sizes of 1 cm x 1cm have been cleaned with ethanol in a digital ultrasonic cleaner device (model / CD-4820) for 15 minutes. Next, these substrates were rinsed with distilled water. After that, they were dried at room temperature and placed on the anode in the deposition chamber. However, it can be directly heated by an electrical heater as another way for drying to eject all impurities. Plasma in the deposition chamber was generated by the glow discharge of argon gas at a maximum pressure of 1.5 mbar and a flow rate of 500 SCCM. The separation between the cathode and the anode was 7 cm. A discharge current of 15 mA was used in this work. A rotary pump has been used to discharge the tube to a vacuum below the 2.4 10^{-2} mbar. To investigate the sputtering time effect on the formation of the particles, the experiment ran for 5 and 10 minutes, while the time 30 minutes was to investigate XRD patterns. The optical properties represented by the prepared samples' reflectance were analyzed using (AvoSpec-2048). While the structural properties of the deposited Ti thin films were taken using a (Phillips- Xpert) x-ray diffractometer with (λ=1.54056 Å) as well as field emission scanning electron microscopy (FE-SEM) (Carl Zeiss Auriga).

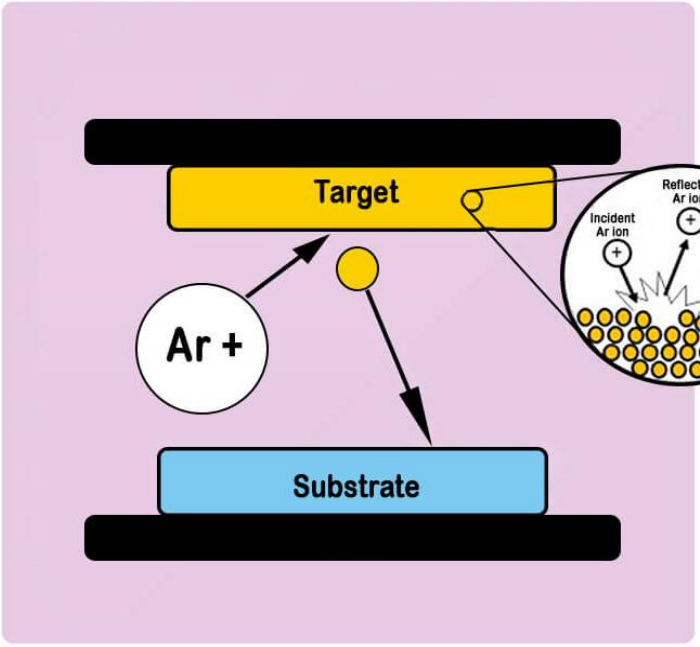

Figure 1: Scheme of DC diode sputtering system.

3. Results and Discussion

The thickness of the prepared thin films has been obtained using an optical interferometer technique. This technique is based on the interference of light beams reflected from the thin film surface and substrate bottom. The diode laser of wavelength (532 nm) has been used, and the thickness is determined using the formula:

$$\boldsymbol{d} = \frac{\boldsymbol{\Delta x}}{\boldsymbol{x}} \times \frac{\boldsymbol{\lambda}}{\boldsymbol{2}} \quad (1)$$

Where x is the Fringe width, Δx is the distance between two fringes and λ is the Wavelength of laser light.

X-ray diffraction patterns are shown in Figure 2 at the range of $2\theta \approx 20°$ to $60°$ for the Ti thin films obtained by DC diode sputtering on glass and n-type Si substrates. XRD peaks for Ti thin films on the glass substrate were shown at $2\theta \sim 35°$ and $38°$ on the (1 0 0) and (0 0 2) planes, respectively. The same peaks have been seen for Ti thin films on n-type Si substrate and (10 1) plane that showed at $2\theta \sim 40°$ according to standards (JCPDS 00-044-1294) as in [34]. So, the reason for disappearing some Ti patterns from the XRD results may be to return to the thermal stress induced in the thin film. From Figure 2, we can indicate that the prepared thin films on glass and n-type Si showed high peak intensity over the plane (0 0 2). The (0 0 2) is the preferential plane for thin-film growth on these substrates. Figure 2 reveals the hexagonal structure of the prepared titanium thin films. The effect of the substrate type on XRD patterns of titanium thin films was clearly shown in Figure 2. The grain size and dislocation density were changed due to the substrate type. The growth of TiNPs on glass substrate exhibited greater grain size than that deposited on Si n-type substrate, which agrees with previous research work of Francisco et. al [35]. The Scherrer formula was used to determine the grain size of the titanium thin film (D) [36].

$$\boldsymbol{D} = \boldsymbol{K}.\frac{\boldsymbol{\lambda}}{\boldsymbol{\beta.cos\theta}} \quad (2)$$

Where K is the shape factor of the average grain (0.9), λ is the X-ray wavelength (0.154056 nm for Cu Kα1), β is the full width at half maximum of the diffraction peak in radians, θ is the diffraction peak angle. From Eq. (2), the FWHM of the diffraction peak has an inverse relation to the grain size of the nanoparticles. As the nanoparticle grain size increased, the diffraction peak became sharper. The dislocation density (δ), which represents the length of the dislocation per unit volume of the crystal, can be determined from formula (3):

$$\boldsymbol{\delta = 1/D2} \tag{3}$$

Thin-film parameters from XRD results are presented in Table 1. The surface morphology of the prepared films was identified using FE-SEM. Figure 3 shows similar, isolated granular surface shape morphology with uniform distribution of TiNPs prepared in this work. These nanoparticles were homogeneously distributed on the substrate surfaces. These images confirmed that, in a specific area, the distribution of granules that form the crystals was increased with the increase of sputtering time. For the prepared samples in 10 min, fewer surfaces of the glass and Si can be observed. Figure 4 shows the EDX mode of the FESEM analysis of titanium nanostructures synthesized on different substrates at different sputtering times. The EDX spectrum of each element composition was almost similar, except the weight of the elements was different due to the change in the sputtering time. For TiNPs deposited on a glass substrate, approximately 18.3% and 31.1% weight of titanium was present in the prepared nanoparticles for 5 and 10 min respectively, while TiNPs deposited on n-type Si substrate about 25.7% and 38.8% weight. The other percentages were for other elements, as shown in Figure 4. The histogram of Ti nanoparticles on glass at 5 min; Figure 5 (a), (b) changes from 10 - 190 nm, with a peak at 70 nm when deposition time rose to 10 min; Figure 5 (b), the peak will be at 100 nm. While the histogram of Ti nanoparticles on Si (n-type) at 5 min; Figure 5 (c), results in nanoparticles dimensions varying between 5 - 65 nm, with a peak at 10 nm. Increasing the deposition time to 10 min, Figure 5 (d), the Ti nanoparticles will be varied between 12 - 120 nm with a peak at 24 nm. The reflectivity measurements as a function of the sputtering time, depending on the reflectivity peak at the reference wavelength (Sodium line) 589 nm. Si is about (29%) based on the dielectric constant value and the refractive index for the bulk.

$$\mathbf{n=}\sqrt{\boldsymbol{\mathcal{E}r}} \tag{4}$$

Where $\mathcal{E}r$ is about 11.7, n=3.4 at the air/Si interface, the reflectivity R= 29% according to:

$$\mathbf{R=}\left(\frac{\boldsymbol{n2-n1}}{\boldsymbol{n2+n1}}\right)^{\mathbf{2}} \tag{5}$$

While for the plasmonics Ti/Si, the reflectivity of this combination is 16.38% and 13.09% for sputtering time 5 min and 10 min, respectively as shown in Figure 6. From these measurements, the deposition of a metallic nanolayer on Si decreased reflectivity, especially at the 10-min sample, the lower curve in Figure 6. This will create a new understanding of reflectivity, where the plasmonic nanoparticles play an important role in decreasing reflectivity. Each plasmonics nanoparticle will act as a localized fabryperot between the surface of the based Si and the plasmonics layer. This will increase the possibility of photon absorption, which implies a reduction in reflectivity based on the scientific fact that the R+T+A=1. The increasing absorption in the plasmonics regime is strongly related to the sizes of metallic nanoparticles.

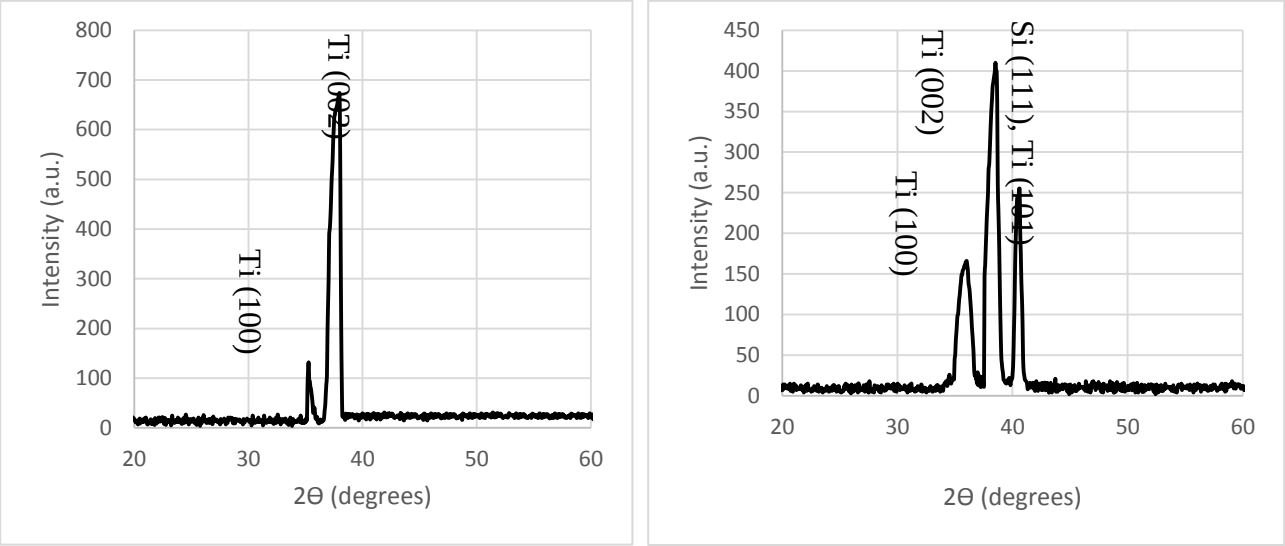

Figure 2: XRD patterns of Ti nanoparticles (a) on glass substrate and (b) on Si (n-type) at 30 min.

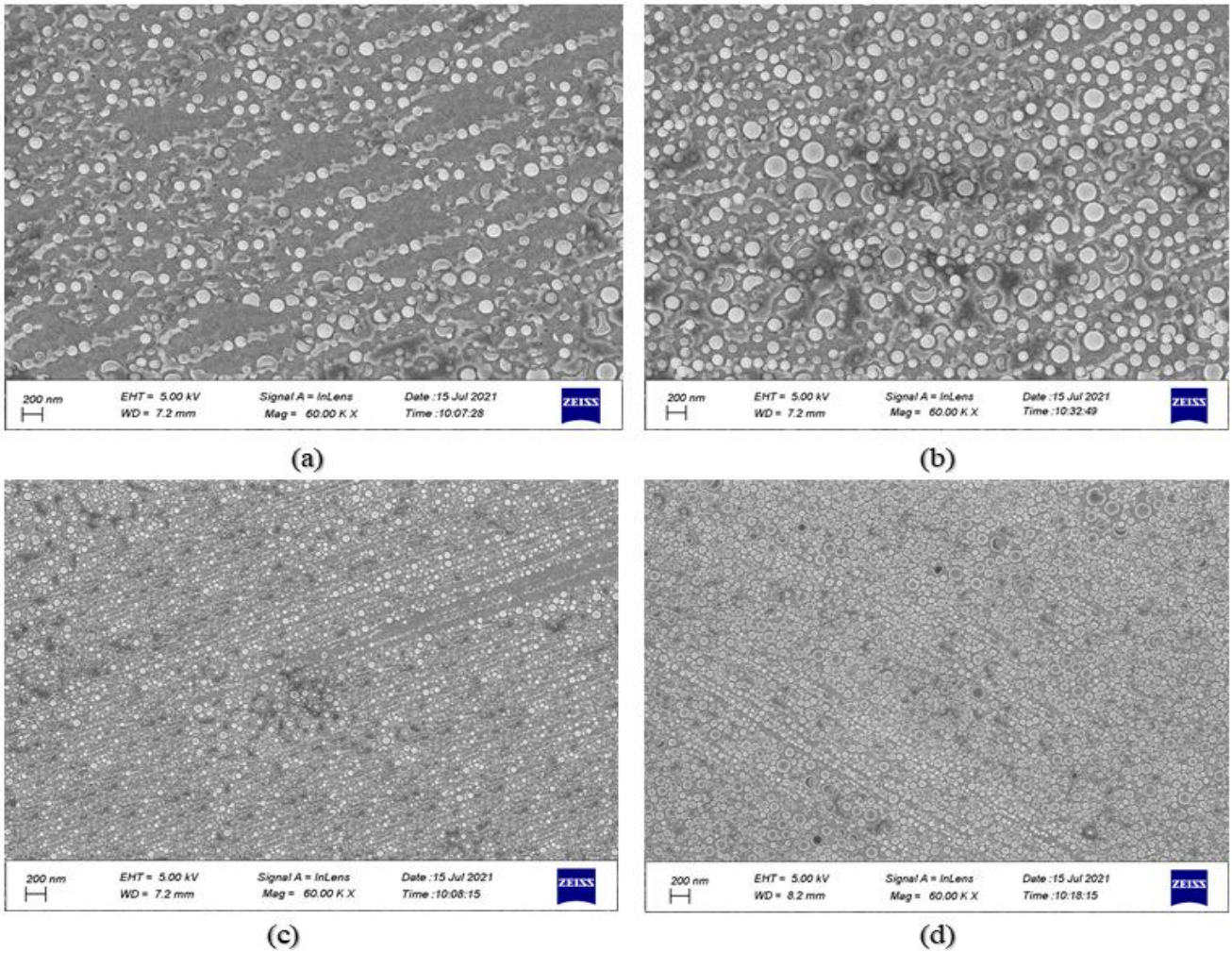

Figure 3. FE-SEM of Ti nanoparticles at 5and 10 min (a,b) on glass substrate and (c,d) on Si (n-type).

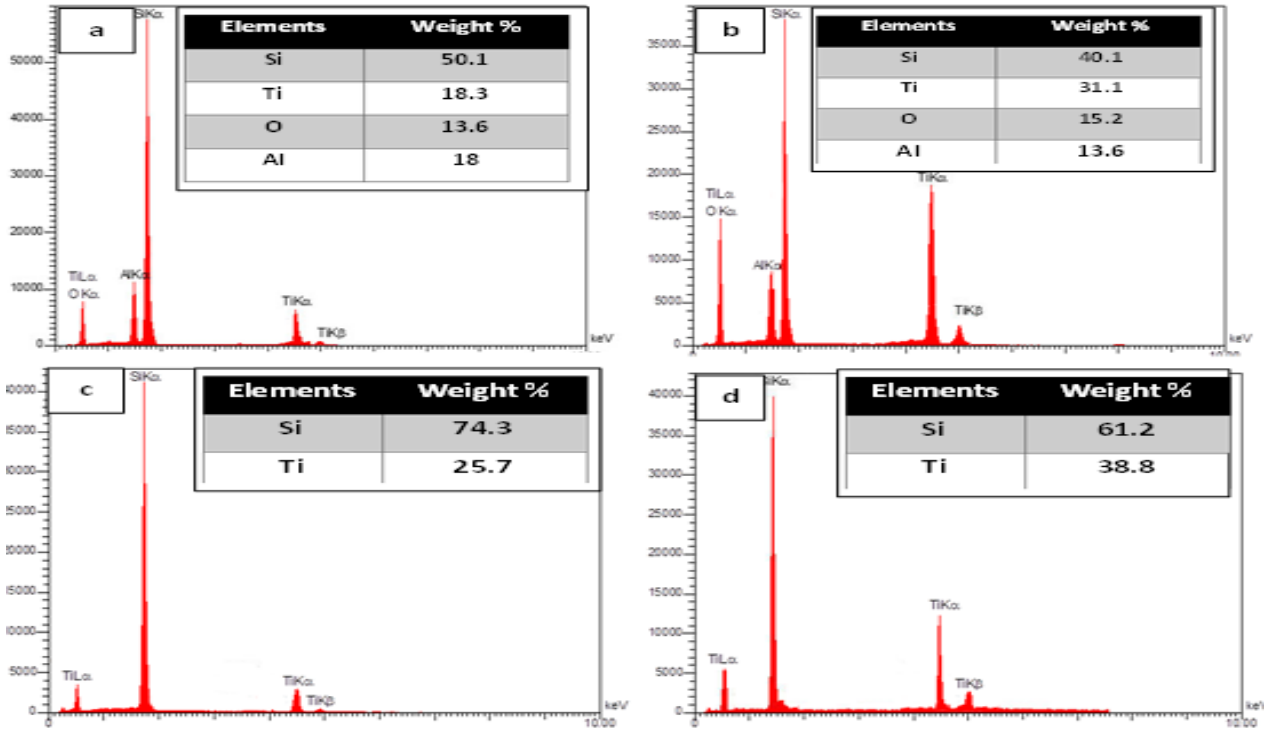

Figure 4: EDX of Ti nanoparticles at 5&10 min (a,b) on glass substrate and (c,d) on Si (n-type).

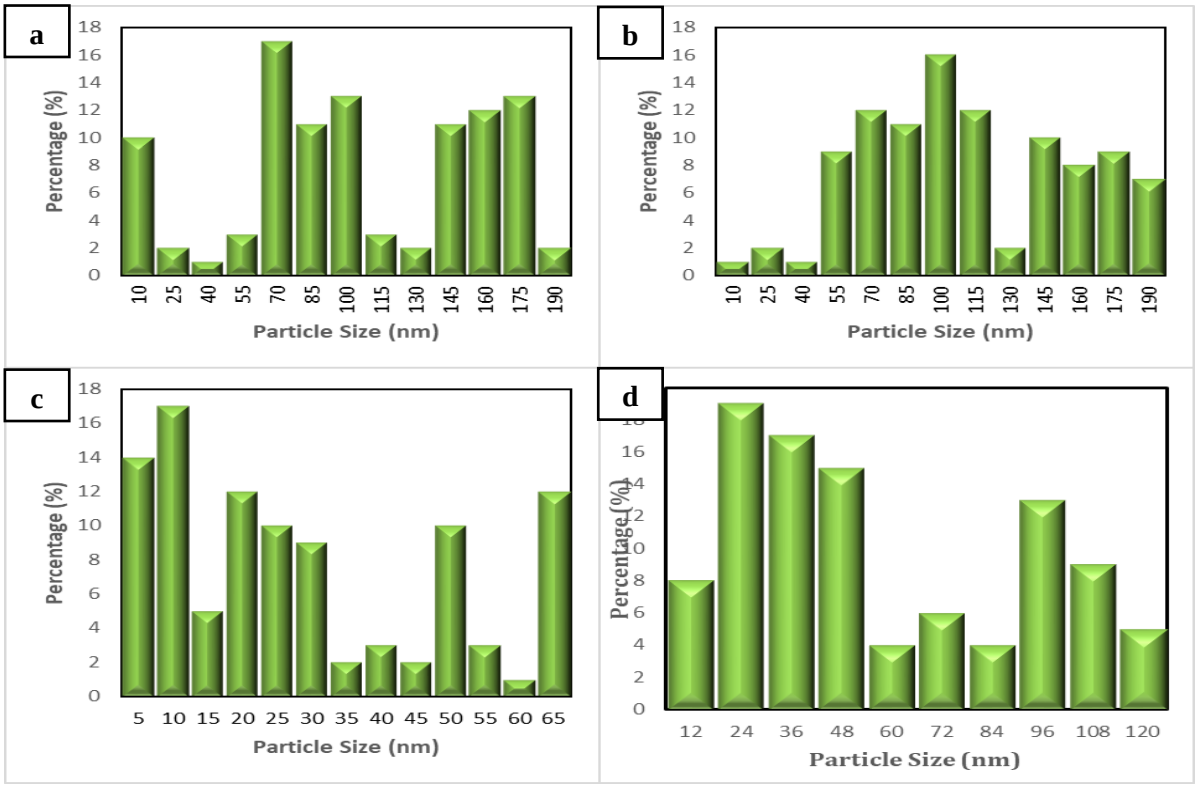

Figure 5: Histogram of Ti nanoparticles size at 5&10 min (a,b) on glass substrate and (c,d) on Si (n-type).

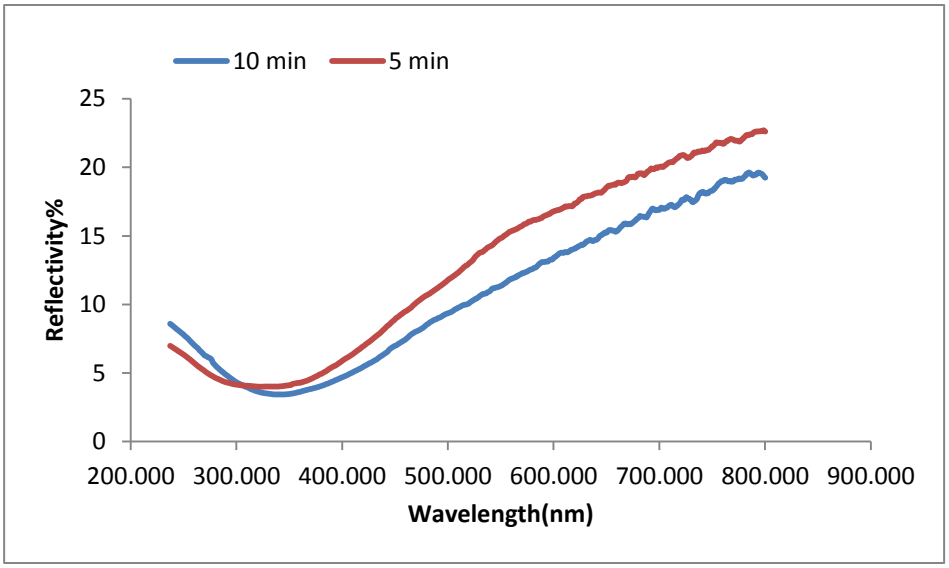

Figure 6: Reflectance spectra of Ti nanoparticles on Si (n-type) substrate at 5 min & 10 min.

Table 1. XRD parameter of Ti thin films on glass and Si (n-type).

Substrate type	(h k l)	2θ(degree)	FWHM(rad)	D(nm) =0.9λ/βcosθ	$\delta=1/D^2(cm^{-2})$
glass	(100)	35	0.015	9.7	1.1E+12
	(002)	38	0.018	8.08	1.53E+12
Si (n-type)	(100)	35	0.016	8.7	1.30E+12
	(002)	38	0.020	7.3	1.87E+12
	(101)	40	0.014	10.3	9.4E+11

4. Conclusions

An efficient reduction in the surface reflectivity was achieved in this work by incorporating plasmonics TiNPs. The obtained results refer to the ability to use plasmonics NPs in applications such as an anti-reflection layer. The effect of sputtering time and substrate type was investigated in this paper. The Ti thin films thickness increases lightly with the sputtering time. The results from XRD revealed that Ti's hexagonal structure successfully grows on glass and n-Si (111) substrates via the DC diode sputtering process. According to Ti (002) peak intensity, the grain size of Ti NPs deposited on glass substrate was higher than that deposited on n-type Si. The surface morphologies of the Ti thin films indicated the formation of a granular surface when Ti is deposited on glass and n-type Si (111) substrate. The prepared thin films exhibit preferred orientation along the (0 0 2) plane.

Acknowledgment

The authors thank the Applied Sciences department at the University of technology-Iraq for providing access to laboratories.

Conflict of Interest

The authors would like to declare that they have no conflict of interest.

References

[1] N. Jackson, R. O'Keefe, F.Waldron, M. O'Neill, A. Mathewson, "Infuence of aluminum nitride crystal orientation on MEMS energy harvesting device performance," *J. Micromech. Microeng*,vol. 23(7), pp. 1–9, 2013.

[2] K. Shaima, A. Saad, A. Omar, "Study of the Partial Shading Effect on the Performance of Silicon PV Panels String," *Journal of Applied Sciences and Nanotechnology*, vol. 1, pp. 32-42, 2021.

[3] M. Kadhim, A. Hasan, M. Akraa, and A. Layla, "Preparation and optimization of heterojunction donor (DLC)–acceptor (SI) as a solar cell by DFT and PLD," *Journal of Ovonic Research*, Vol, 17(3), PP. 273-281, 2021.

[4] A. Hasan, F. Mohammed, and M. Takz, "Design and Synthesis of Graphene Oxide-Based Glass Substrate and Its Antimicrobial Activity Against MDR Bacterial Pathogens," *Journal of Mechanical Engineering Research and Developments*, vol. 43, pp. 11-17, 2020.

[5] A. Haider, Z. Jameel, I. Al-Hussaini, "Review on: titanium dioxide applications," *Energy Procedia*, vol. 157, pp. 17-29, 2019.

[6] A. Hasan, B. Kadem, M. Akraa, and A. Hassan, "PVA: PEDOT: PSS: Carbon BASED nano-composites for pressure sensor applications*," Digest Journal Of Nanomaterials And Biostructures*, vol. 15(1), pp. 197-205, 2020.

[7] F. Mohammed, M. Edan, A. Hasan, and A. Haider, "Synthesis and Theoretical Concepts of Boron Nitride Nanowires Grown on Nitrides Stainless Steel Surface by Hybrid Gas Phase Process," *In Key Engineering Materials*, Vol. 886, pp. 97-107, 2021.

[8] G. Iriarte, J. Bjurstrom, J. Westlinder, F. Engelmark, and I. Katardjiev, "Synthesis of C-axis-oriented AlN thin flms on highconducting layers_Al, Mo, Ti, TiN, and Ni. IEEE Trans. Ultrason. Ferroelectr," *Freq. Control*, vol. 52(7), pp. 1170–1174, 2005.

[9] K. Adam, I. Atheer, R. Mohammad, "Preparation and Characterization of Electron Transfer Layer for Perovskite Solar Cells," *Journal of Applied Sciences and Nanotechnology*, vol. 1, pp. 58-63, 2021.

[10] Y. Li, C. Yang, H. Zhao, S. Qu, X. Li, and Y. Li, "New Developments of Ti-Based Alloys for Biomedical Applications," *Materials*, vol.7, pp.1709-1800, 2014.

[11] D. Kim, J. Kwon, G. Jang, and N. Hwang, "Effect of Pressure on the Film Deposition during RF Magnetron Sputtering Considering Charged Nanoparticles," *Coatings*, vol. 11, p. 132, 2021.

[12] C. Sanchez, B. Rebollo, M. Maia, and F. Freire, "Titanium diboride thin films produced by dc-magnetron sputtering: Structural and mechanical properties," *Surface and Coatings Technology*, Vol. 205, pp. 3698-3702, 2011.

[13] A. Demortière, A. Snezhko, M. Sapozhnikov, N. Becker, T. Proslier, and I. Aranson, "Self-assembled tunable networks of sticky colloidal particles," *Nat. Commun*. Vol. 5, p. 3117, 2014.

[14] J. Ferrar and M. Solomon, "Kinetics of colloidal deposition, assembly, and crystallization in steady electric fields," *Soft Matter* vol. 11, pp. 3599–3611, 2015.

[15] Z. Wang, B. He, G. Xu, G. Wang, J. Wang, Y. Feng, D. Su, B. Chen, H. Li, and Z. Wu et al, "Transformable masks for colloidal nanosynthesis," *Nat. Commun*., vol. 9, p. 563, 2018.

[16] A. Reem, Odai N., O. Mohammed O., "Physical Investigations of Titanium Dioxide Nanorods Film Prepared by Hydrothermal Technique," *Journal of Applied Sciences and Nanotechnology*, vol. 1, pp. 32-41, 2021.

[17] D. Kim and N. Hwang, "Synthesis of nanostructures using charged nanoparticles spontaneously generated in the gas phase during chemical vapor deposition," *J. Phys. D Appl. Phys*., Vol. 51, p. 463002, 2018.

[18] N. Hwang, "Non-Classical Crystallization of Thin Films and Nanostructures in CVD and PVD Processes," *Springer Netherlands*: Dordrecht, Vol. 60, pp. 1–332, 2016.

[19] V. Chawla, R. Jayaganthan, A. Chawla, and R. Chandra, "Morphological study of magnetron sputtered Ti thin flms on silicon substrate," *Mater. Chem. Phys*., Vol. 111, pp. 414–418, 2008.

[20] V. Chawla, R. Jayaganthan, A. Chawla, and R. Chandra, "Microstructural characterizations of magnetron sputtered Ti flms on glass substrate, " *J. Mater. Process. Technol*., Vol. 209, pp. 3444–3451, 2009.

[21] A. Chen, Y. Bu, Y. Tang, Y. Wang, F. Liu, X. Xie, and J. Gu, "Deposition-rate dependence of orientation growth and crystallization of Ti thin flms prepared by magnetron sputtering," *Thin Solid Films*, vol. 574, pp. 71–77, 2015.

[22] Y. Jeyachandran, B. Karunagaran, S. Narayandass, and D. Mangalaraj, "The effect of thickness on the properties of titanium flms deposited by dc magnetron sputtering," *Mater. Sci. Eng*., A, vol. 458, pp. 361–365, 2007.

[23] Y. Tetsu and O. Nittono, "Microstructure and preferred orientation in pure titanium films deposited by two-facing-targettype dc sputtering," *Thin Solid Films*, vol. 281, pp. 128–131, 1996.

[24] J. Kwon, D. Kim, and N. Hwang, "Generation of Charged Ti Nanoparticles and Their Deposition Behavior with a Substrate Bias during RF Magnetron Sputtering," *Coatings*, vol. 10, p. 443, 2020.

[25] L. Maissel and P. Schaible, "Thin films deposited by bias sputtering," *J. Appl. Phys*., Vol. 36, pp. 237–242, 1965.

[26] K. Wasa, I. Kanno, and H. Kotera, "Handbook of Sputter Deposition Technology," Book Second Edition, 2012.

[27] H. Yu, Y. Peng, and Y. Yang, "Plasmon-enhanced light–matter interactions and applications," *npj Comput Mater*, vol. 5, p. 45, 2019.

[28] E. Petryayeva, and U. Krull, "Localized surface plasmon resonance: nanostructures, bioassays and biosensing," *Anal Chim Acta*. vol. 7, pp. 8-24, 2011.

[29] X. Zhang, J. Shao, Ch. Yan, R. Qin, Z. Lu, H. Geng, T. Xu, and L. Ju, "Optoelectronic device applications of 2D transition metal carbides and nitrides," *Materials & Design*, vol. 200, 2021.

[30] A. Haider, A. Najim, M. Muhi, "*TiO2/Ni composite as antireflection coating for solar cell application*," Optics Communications, vol. 370, pp. 263-266, 2016.

[31] V. Janković, Y. Yang, J. You et al, "Active layer-incorporated, spectrally tuned Au/SiO2 core/shell nanorod-based light trapping for organic photovoltaics," *ACS Nano*. vol. 7, pp. 3815–3822, 2013.

[32] P. Banerjee, D. Conklin, S. Nanayakkara et al, "Plasmon-induced electrical conduction in molecular devices," *ACS Nano*, vol. 4, pp. 1019–1025, 2010.

[33] M. Kwon, J. Kim, and B. Kim et al, "Surface-plasmon1enhanced light-emitting diodes," *Adv Mater*, vol. 20, pp. 1253–1257, 2008.

[34] M. Perillo and F. Daniel, "Formation of TiO2 Nanopores by Anodization of Ti-Films," *Open Access Library Journal*, vol. 1, pp. 1-9, 2014.

[35] X. Zhu, G. Peng, W. Haihua, D. Yang, H. Sun, P. Wangyang, L. Jitao, and H. Tian, "Influence of substrate on structural, morphological and optical properties of TiO_2 thin films deposited by reaction magnetron sputtering," *AIP Advances*, vol. 7, p. 125326, 2017.

[36] M. Francisco, M. Felipe, H. Paulo, F. Ana, and N. Francisco, "Nanostructured titanium dioxide average size from alternative analysis of Scherrer's Equation," *revista Matéria*, 23(1), 2018.